J. Fluid Mech. (1997), *vol.* 332, *pp.* 395–409

Analogy between predictions of Kolmogorov and Yaglom

By R. A. ANTONIA[1], M. OULD-ROUIS[2], F. ANSELMET[2] AND Y. ZHU[1]

[1]Department of Mechanical Engineering, University of Newcastle, NSW, 2308, Australia
[2]Institut de Recherche sur les Phénomènes Hors Équilibre, Université d'Aix-Marseille II, 13003 Marseille, France

(Received 22 April 1996 and in revised form 9 September 1996)

The relation, first written by Kolmogorov, between the third-order moment of the longitudinal velocity increment δu_1 and the second-order moment of δu_1 is presented in a slightly more general form relating the mean value of the product $\delta u_1(\delta u_i)^2$, where $(\delta u_i)^2$ is the sum of the square of the three velocity increments, to the second-order moment of δu_i. In this form, the relation is similar to that derived by Yaglom for the mean value of the product $\delta u_1(\delta\theta)^2$, where $(\delta\theta)^2$ is the square of the temperature increment. Both equations reduce to a 'four-thirds' relation for inertial-range separations and differ only through the appearance of the molecular Prandtl number for very small separations. These results are confirmed by experiments in a turbulent wake, albeit at relatively small values of the turbulence Reynolds number.

1. Introduction

Starting with the Kármán–Howarth (1938) equation, Kolmogorov (1941) wrote an equation relating third-order moments of the longitudinal velocity increment $\delta u_L \equiv u_L(\boldsymbol{x}) - u_L(\boldsymbol{x}_0)$ to second-order moments of δu_L where the subscript L indicates the direction of the separation vector $\boldsymbol{r}$ $(= \boldsymbol{x} - \boldsymbol{x}_0)$. If u_L and $r = |\boldsymbol{r}|$ are identified with u_1 and r_1, the x_1 components of $\tilde{u}$ $(\equiv u_i)$ and $\boldsymbol{r}$ $(\equiv r_i)$, the equation may be written as

$$\langle(\delta u_1)^3\rangle = 6\nu\frac{\mathrm{d}}{\mathrm{d}r_1}\langle(\delta u_1)^2\rangle - \tfrac{4}{5}\langle\epsilon\rangle r_1, \tag{1.1}$$

where $\langle\epsilon\rangle$ is the mean dissipation rate of the turbulent kinetic energy (angular brackets denote ensemble averages), ν is the kinematic viscosity of the fluid. Strictly, (1.1) is not exact for isotropic turbulence with zero mean velocity since it lacks both an unsteady term (decaying turbulence) and a forcing term (to maintain a statistically steady state). The correct form of the equation for decaying turbulence was given in Batchelor (1947) and Landau & Lifshitz (1959); see also Lindborg (1996). In his treatment of what he calls the Kármán–Howarth–Monin relation, Frisch (1995) included a random forcing term, active only at large scales, which is stationary in time and homogeneous in space. The contribution of this term to (1.1) is expected to be small when r_1 is small compared with the length scale of the force and the Reynolds number is sufficiently large (Nelkin 1994). Monin (1959) relaxed the assumption of isotropy used in (1.1), to one of local isotropy (see Monin & Yaglom 1975). However Lindborg (1996) has shown that the pressure-velocity correlation terms are

erroneously omitted on p. 402 of Monin & Yaglom. The relaxation is evidently important since the validity of (1.1) now hinges only on the small-scale structure of the turbulence being isotropic, an expectation which seems reasonable when the Reynolds number is sufficiently large. In the inertial range ($\eta \ll r_1 \ll L$, where η and L are the Kolmogorov and integral length scales respectively), (1.1) reduces to

$$\langle(\delta u_1)^3\rangle = -\tfrac{4}{5}\langle\epsilon\rangle r_1 \tag{1.2}$$

which is sometimes referred to as the 'four-fifths' law (e.g. Vainshtein & Sreenivasan 1994). In the limit $r_1 \to 0$, (1.1) can be reduced, after applying a Taylor series expansion about $r_1 = 0$, and ignoring terms of order (r^4) or greater, to

$$\left\langle \left(\frac{\partial u_1}{\partial x_1}\right)^3 \right\rangle = -2\nu \left\langle \left(\frac{\partial^2 u_1}{\partial x_1^2}\right)^2 \right\rangle. \tag{1.3}$$

Relation (1.3) represents the isotropic form of the equality between the production of vorticity through vortex stretching and the viscous diffusion of vorticity. In isotropic turbulence, $\langle\epsilon\rangle$ is given by

$$\langle\epsilon\rangle = 15\nu \left\langle \left(\frac{\partial u_1}{\partial x_1}\right)^2 \right\rangle. \tag{1.4}$$

There has been significant experimental support for both (1.2) and (1.3) in globally anisotropic shear flow turbulence, with $\langle\epsilon\rangle$ estimated via relation (1.4) (e.g. Monin & Yaglom 1975). Further, (1.2) and (1.3) have been verified not only at atmospheric values of the turbulence Reynolds number R_λ but also when R_λ is quite small. The earliest verification of (1.3) is due to Batchelor & Townsend (1947) in grid turbulence with R_λ in the range 20–60. In theory, one would not have expected local isotropy to be a good approximation at small R_λ; in fact, Durbin & Speziale (1991) have suggested that local isotropy is strictly not consistent with the Navier–Stokes equations even at infinitely large R_λ when the mean shear is not zero. In practice, isotropy appears to be closely approximated by the smallest scales when the shear is small (e.g. Kim & Antonia 1993; Antonia & Kim 1994). Equation (1.1) has received experimental support with r_1 varying between η and inertial-range scales for similar values of R_λ for which (1.2) and (1.3) have been verified. Although there is experimental evidence which suggests that (1.1), (1.2) and (1.3) are not satisfied when local isotropy is violated, for example in near-wall turbulence, their verification for small R_λ requires some investigation. A possible reason may be that these relations are not sensitive tests of local isotropy; alternatively, it may be argued that local isotropy is only a weak assumption.

The previous considerations have led us to re-examine the assumptions needed to arrive at (1.2) and (1.3). An equation for $\langle\delta u_1(\delta u_i)^2\rangle$ (repetition of indices implies summation) is derived in §2. It is noted that this equation bears a close analogy to Yaglom's (1949) equation

$$\langle\delta u_1(\delta\theta)^2\rangle = 2\kappa\frac{\partial}{\partial r_1}\langle(\delta\theta)^2\rangle - \tfrac{4}{3}\langle\epsilon_\theta\rangle r_1, \tag{1.5}$$

where θ is the instantaneous temperature fluctuation and $\delta\theta$ is the temperature increment $\theta(\boldsymbol{x}) - \theta(\boldsymbol{x}_0)$. In (1.5), κ is the thermal diffusivity and $\langle\epsilon_\theta\rangle$ is the mean

dissipation rate for $\langle\theta^2\rangle/2$ which, for isotropic turbulence, is given by

$$\langle\epsilon_\theta\rangle = 3\kappa\left\langle\left(\frac{\partial\theta}{\partial x_1}\right)^2\right\rangle. \tag{1.6}$$

The assumptions embodied in (1.5) are briefly considered in §3. In the inertial range, (1.5) reduces to

$$\langle(\delta u_1)(\delta\theta)^2\rangle = -\tfrac{4}{3}\langle\epsilon_\theta\rangle r_1. \tag{1.7}$$

i.e. a 'four-thirds' law. When $r_1 \to 0$, (1.5) becomes, by applying a Taylor series expansion about $r_1 = 0$ and ignoring terms greater than or equal to order (r_1^4),

$$\left\langle\left(\frac{\partial u_1}{\partial x_1}\right)\left(\frac{\partial\theta}{\partial x_1}\right)^2\right\rangle = -\frac{2}{3}\kappa\left\langle\left(\frac{\partial^2\theta}{\partial x_1^2}\right)^2\right\rangle, \tag{1.8}$$

which expresses a balance between the production of ϵ_θ due to the stretching of the temperature gradient field by the turbulent strain field and the dissipation rate or molecular smoothing of the temperature gradient field (Wyngaard 1971).

The analogy between the equation for $\langle\delta u_1(\delta u_i)^2\rangle$ and (1.5) follows from the analogous forms of the transport equations for $\langle(\delta u_i)^2\rangle$ and $\langle(\delta\theta)^2\rangle$ or, as was pointed out by Fulachier (1972) (also, Fulachier & Dumas 1976, and Fulachier & Antonia 1984) the similarity between the transport equations for the two-point correlations $\langle u_i(\boldsymbol{x})u_i(\boldsymbol{x}_0)\rangle$ and $\langle\theta(\boldsymbol{x})\theta(\boldsymbol{x}_0)\rangle$. Experimental verification for the analogous forms of (1.7) and (1.8), obtained by replacing θ by u_i and κ by ν, is provided in §5 and §6 respectively, using measurements in a turbulent wake.

2. Third-order velocity structure function

We start with the incompressible Navier–Stokes equations at points $\boldsymbol{x}$ and $\boldsymbol{x}_0$:

$$\partial_t u_i + u_\alpha\partial_\alpha u_i = -\partial_i p + \nu\partial_\alpha^2 u_i, \tag{2.1}$$

$$\partial_t u_{0i} + u_{0\alpha}\partial_{0\alpha}u_{0i} = -\partial_{0i}p_0 + \nu\partial_{0\alpha}^2 u_{0i}, \tag{2.2}$$

where u_i and u_{0i} are the instantaneous velocities at $\boldsymbol{x}$ and $\boldsymbol{x}_0$, p and p_0 are the kinematic pressures at $\boldsymbol{x}$ and $\boldsymbol{x}_0$, $\partial_t \equiv \partial/\partial t$, $\partial_\alpha \equiv \partial/\partial x_\alpha$, $\partial_{0\alpha} \equiv \partial/\partial x_{0\alpha}$ and ∂_α^2 is the Laplacian $\partial^2/\partial x_\alpha^2$. Recalling that u_i depends only on $\boldsymbol{x}$ and u_{0i} depends only on $\boldsymbol{x}_0$, subtraction of (2.2) from (2.1) and re-arrangement of some of the terms yields an equation for the velocity increment $\delta u_i \equiv u_i - u_{0i}$:

$$\partial_t\delta u_i + \delta u_\alpha\frac{\partial(\delta u_i)}{\partial r_\alpha} + u_{0\alpha}(\partial_\alpha + \partial_{0\alpha})\delta u_i = -(\partial_i + \partial_{0i})\delta p + \nu(\partial_\alpha^2 + \partial_{0\alpha}^2)\delta u_i. \tag{2.3}$$

The third term on the left-hand side is absent in (22.14) of Monin & Yaglom (1975), in which the left-hand side is written with respect to a moving frame of reference whilst the right-hand side is with respect to a fixed frame of reference. All terms in (2.3) are for the same fixed reference frame.

In general, the velocity increment δu_i depends on the separation $r_i \equiv x_i - x_{0i}$ and time t. Multiplying (2.3) with $2\delta u_i$ and averaging, and noting that $4\langle\delta u_i\partial_\alpha^2\delta u_i\rangle = 2\langle\partial_\alpha^2(\delta u_i)^2\rangle - 4\langle(\partial_\alpha u_i)^2\rangle$ results in

$$\frac{\partial}{\partial t}\langle(\delta u_i)^2\rangle + \frac{\partial}{\partial r_\alpha}\langle\delta u_\alpha(\delta u_i)^2\rangle = 2\nu\frac{\partial^2}{\partial r_\alpha^2}\langle(\delta u_i)^2\rangle - 4\nu\langle(\partial_\alpha u_i)^2\rangle - 2\langle\delta u_i(\partial_i + \partial_{0_i})\delta p\rangle. \tag{2.4}$$

In arriving at (2.4), we have used the fact that x_i and x_{0i} are independent; homogeneity and incompressibility have also been used. The pressure term is zero because

$$\langle \delta u_i(\partial_i + \partial_{0_i})\delta p\rangle = \langle \partial_i(\delta u_i \delta p)\rangle + \langle \partial_{o_i}(\delta u_i \delta p)\rangle$$

and, since $\partial_i \equiv \partial/\partial r_i$ and $\partial_{0i} \equiv -\partial/\partial r_i$ when applied to two-point averages, the terms on the right-hand side of the above equality cancel each other (a slightly different approach was used by Hinze (1959) for eliminating the pressure term, see p. 259). Order of magnitude arguments suggest that the first term on the left-hand side of (2.4) becomes negligible compared with the other terms in that equation when the Reynolds number increases (e.g. Lindborg 1996). With these simplifications, (2.4) reduces to

$$\frac{\partial}{\partial r_\alpha}\langle \delta u_\alpha (\delta u_i)^2\rangle = 2\nu \frac{\partial^2}{\partial r_\alpha^2}\langle (\delta u_i)^2\rangle - 4\nu \langle (\partial_\alpha u_i)^2\rangle. \tag{2.5}$$

Since $\nu\langle(\partial_\alpha u_i)^2\rangle$ can be identified with the average turbulent energy dissipation rate $\langle\epsilon\rangle$ and $-4\langle\epsilon\rangle \equiv -\frac{4}{3}\partial(\langle\epsilon\rangle r_\alpha)/\partial r_\alpha$, (2.5) becomes

$$\frac{\partial}{\partial r_\alpha}\langle \delta u_\alpha (\delta u_i)^2\rangle = 2\nu \frac{\partial^2}{\partial r_\alpha^2}\langle (\delta u_i)^2\rangle - \frac{4}{3}\frac{\partial}{\partial r_\alpha}(\langle\epsilon\rangle r_\alpha). \tag{2.6}$$

Equation (2.5) is identical to (22.15) in Monin & Yaglom (written here using the present notation)

$$\frac{\partial}{\partial r_k}\langle (\delta u_i \delta u_j \delta u_k)\rangle = 2\nu \frac{\partial^2}{\partial r_k^2}\langle \delta u_i \delta u_j\rangle - \tfrac{4}{3}\langle\epsilon\rangle\delta_{ij}$$

after applying the contraction $i = j$. It should be noted that Frisch (1995) has derived a similar result (equation 6.8, p. 78) except for the inclusion of a random forcing function term. In the inertial range, Frisch obtains (using our notation)

$$-\frac{1}{4}\frac{\partial}{\partial r_\alpha}\langle (\delta u_i)^2 \delta u_\alpha\rangle = \langle\epsilon\rangle,$$

which is equivalent to (2.6) when ν is neglected.

Equation (2.6) can now be projected onto the x_1-direction using isotropy. The result is

$$\left(\frac{2}{r_1} + \frac{\partial}{\partial r_1}\right)\langle \delta u_1 (\delta u_i)^2\rangle = \left(\frac{2}{r_1} + \frac{\partial}{\partial r_1}\right)\left[2\nu\frac{\partial}{\partial r_1}\langle (\delta u_i)^2\rangle - \tfrac{4}{3}\langle\epsilon\rangle r_1\right]. \tag{2.7}$$

As was noted by Kármán & Howarth (1938) – see also Monin & Yaglom (p. 122) – the only solution of the equation

$$\left(\frac{2}{r_1} + \frac{\partial}{\partial r_1}\right) f(r_1) = 0$$

which has no singularity at $r_1 = 0$ is $f(r_1) = 0$. The solution of (2.7) is then

$$\langle \delta u_1 (\delta u_i)^2\rangle = 2\nu\frac{\partial}{\partial r_1}\langle (\delta u_i)^2\rangle - \tfrac{4}{3}\langle\epsilon\rangle r_1. \tag{2.8}$$

In the inertial range, (2.8) reduces to

$$\langle \delta u_1 (\delta u_i)^2\rangle = -\tfrac{4}{3}\langle\epsilon\rangle r_1, \tag{2.9}$$

i.e. a 'four-thirds' law similar to (1.7). Note that (2.9) would be identical to (1.7)

if u_i were replaced by θ and ν by κ (recall that for isotropic turbulence $\langle\epsilon\rangle = 3\nu\langle(\partial u_i/\partial x_1)^2\rangle$). In the limit of $r_1 \to 0$, a Taylor series expansion about $r_1 = 0$ can be used to lead to

$$\left\langle \left(\frac{\partial u_1}{\partial x_1}\right)\left(\frac{\partial u_i}{\partial x_1}\right)^2 \right\rangle = -\frac{2}{3}\nu \left\langle \left(\frac{\partial^2 u_i}{\partial x_1^2}\right)^2 \right\rangle. \tag{2.10}$$

This equation would be equivalent to (1.8) when u_i is replaced by θ and ν by κ. For isotropic turbulence, (13.91) in Monin & Yaglom can be used to show that, in the inertial range,

$$\langle \delta u_1 (\delta u_2)^2 \rangle = \langle \delta u_1 (\delta u_3)^2 \rangle = \tfrac{1}{3}\langle (\delta u_1)^3 \rangle, \tag{2.11}$$

and it follows that (2.9) reduces to (1.2). Similarly, (2.10), which applies to the dissipative range, reduces to (1.3) since, for isotropic turbulence,

$$\left\langle \left(\frac{\partial^2 u_2}{\partial x_1^2}\right)^2 \right\rangle = \left\langle \left(\frac{\partial^2 u_3}{\partial x_1^2}\right)^2 \right\rangle = 3\left\langle \left(\frac{\partial^2 u_1}{\partial x_1^2}\right)^2 \right\rangle \tag{2.12}$$

and

$$\left\langle \left(\frac{\partial u_1}{\partial x_1}\right)\left(\frac{\partial u_2}{\partial x_1}\right)^2 \right\rangle = \left\langle \left(\frac{\partial u_1}{\partial x_1}\right)\left(\frac{\partial u_3}{\partial x_1}\right)^2 \right\rangle = \frac{2}{3}\left\langle \left(\frac{\partial u_1}{\partial x_1}\right)^3 \right\rangle. \tag{2.13}$$

Expressions (2.12) and (2.13) can be readily obtained from the sixth-order isotropic tensor forms given in Champagne (1978).

3. Equation for $\langle \delta u (\delta\theta)^2 \rangle$

The development here is kept brief since it is similar to that in §2. We start with the temperature equation, written at points $\boldsymbol{x}$ and $\boldsymbol{x}_0$:

$$\partial_t \theta + u_\alpha \partial_\alpha \theta = \kappa \partial_\alpha^2 \theta, \tag{3.1}$$

$$\partial_t \theta_0 + u_{0\alpha} \partial_{0\alpha} \theta_0 = \kappa \partial_{0\alpha}^2 \theta_0. \tag{3.2}$$

Subtraction of (3.1) from (3.2) yields, after some manipulation, an equation for $\delta\theta$:

$$\partial_t \delta\theta + \delta u_\alpha \partial_\alpha \delta\theta + u_{0\alpha}(\partial_\alpha + \partial_{0\alpha})\delta\theta = \kappa(\partial_\alpha^2 + \partial_{0\alpha}^2)\delta\theta. \tag{3.3}$$

Multiplication with $2\delta\theta$ and averaging results in

$$\partial_t \langle (\delta\theta)^2 \rangle + \frac{\partial}{\partial r_\alpha}\langle \delta u_\alpha (\delta\theta)^2 \rangle + \langle u_{0\alpha}(\partial_\alpha + \partial_{0\alpha})(\delta\theta)^2 \rangle = 2\kappa \frac{\partial^2}{\partial r_\alpha^2}\langle (\delta\theta)^2 \rangle - 4\kappa \langle (\partial_\alpha \delta\theta)^2 \rangle. \tag{3.4}$$

Using arguments similar to those mentioned in the context of simplifying (2.4), equation (3.4) can be simplified to

$$\frac{\partial}{\partial r_\alpha}\langle \delta u_\alpha (\delta\theta)^2 \rangle = 2\kappa \frac{\partial^2}{\partial r_\alpha^2}\langle (\delta\theta)^2 \rangle - 4\kappa \langle (\partial_\alpha \theta)^2 \rangle. \tag{3.5}$$

Since $\kappa\langle(\partial_\alpha\theta)^2\rangle$ can be identified with $\langle\epsilon_\theta\rangle$, the average dissipation rate for $\langle\theta^2\rangle/2$, $4\langle\epsilon_\theta\rangle$ can be replaced by $-\frac{4}{3}\,\partial(\langle\epsilon_\theta\rangle r_\alpha)/\partial r_\alpha$ and (3.5) can be rewritten as

$$\frac{\partial}{\partial r_\alpha}\langle \delta u_\alpha (\delta\theta)^2 \rangle = 2\kappa \frac{\partial^2}{\partial r_\alpha^2}\langle (\delta\theta)^2 \rangle - \frac{4}{3}\,\frac{\partial}{\partial r_\alpha}(\langle \epsilon_\theta \rangle r_\alpha). \tag{3.6}$$

Note that only the assumption of homogeneous turbulence has been used to obtain (3.6). Also, this equation is analogous to (2.6); equations (3.6) and (2.6) would be

d (mm)	x_1/d	U_1 (m s^{-1})	$\langle U\rangle$ (m s^{-1})	R_d	R_λ	η (mm)	θ_K (°C)	$\langle\epsilon\rangle$ (m^2 s^{-3})	$\langle\epsilon_\theta\rangle$ (°C^2 s^{-1})
6.35	240	3.6	3.34	1500	40	0.64	0.01	0.0282	4.3×10^{-3}
25.40	70	14.5	12.9	24500	230	0.14	0.012	8.7	0.113
25.40	70	10.0	9.2	16900	190	0.18	—	2.76	—

TABLE 1. Summary of experimental conditions. x_1 is measured from the cylinder axis, $R_d = U_1 d/\nu$, $R_\lambda = \langle u_1^2\rangle^{1/2}\lambda/\nu$, where $\lambda = \langle U\rangle\langle u_1^2\rangle^{1/2}/\langle(\partial u_1/\partial t)^2\rangle^{1/2}$, $\theta_K = (\langle\epsilon_\theta\rangle\eta/u_K)^{1/2}$, with $u_K = (\nu\langle\epsilon\rangle)^{1/4}$.

identical if u_i, ν and $\langle\epsilon\rangle$ were replaced by θ, κ and $\langle\epsilon_\theta\rangle$ respectively. Equation (1.5) follows from (3.6) by invoking the same procedure that was used to obtain (2.8) from (2.7), i.e. by projecting onto the r_1-direction using isotropy.

4. Experimental details

Measurements of all three velocity fluctuations and of θ were made on the centreline of a turbulent plane wake, of a circular cylinder (diameter d). The floor of the working section was adjusted so that the pressure gradient was zero. Three values of U_1, the free-stream velocity, were used although most of the results presented correspond to $U_1 = 3.6$ m s^{-2} and $U_1 = 14.5$ m s^{-2}; the corresponding experimental conditions are summarized in table 1. Note that, in the context of experimental results, the angular brackets now refer to time-averaged quantities.

At the larger Reynolds number ($R_d = 24\,500$) R_λ was sufficiently large to expect the establishment of a reasonable inertial range, thereby allowing (1.7) and (2.9) to be checked. The smaller Reynolds number ($R_d = 1500$) was selected so as to maximize the magnitude of η, thereby enhancing the ability to resolve the smallest scales; this was needed for checking (1.8) and (2.10).

An X-wire was used to measure the velocity fluctuations u_1, u_2, u_3. Fluctuations u_1 and u_2 were obtained when the X-wire was in the (x_1, x_2)-plane; u_1 and u_3 were determined with the X-wire in the (x_1, x_3)-plane. For all X-wire measurements, the cylinder was at ambient temperature. The fluctuations u_1 and θ were determined simultaneously when the cylinder was heated; the surface temperature was about 120 °C above ambient and the mean temperature at the measurement station was 0.4 °C ($R_d = 1500$) and 0.43 °C ($R_d = 24500$) above ambient. These fluctuations were measured with parallel single wires: a hot wire for u_1 and a cold wire for θ. The longitudinal velocity fluctuation u_1 was measured in a number of different experiments and with different wires; in all cases, the statistics of u_1 and Δu_1 were in good agreement (to within $\pm2\%$) with each other. All the hot wires were of 2.5 μm diameter (Pt–10% Rh) with a nominal length in the range 0.5 to 0.7 mm. They were operated in constant-temperature circuits at an overheat ratio of 0.5. The cold wire had a diameter of 0.63 μm (Pt–10% Rh) and a length of 0.7 mm. It was operated in a constant-current (0.1 mA) circuit.

The signals from the constant-temperature and constant-current circuits were digitized using a 12 bit A-D converter. Prior to digitization, appropriate offset voltages, amplification and low-pass filtering were applied to the signals. For the X-wires, the filter cut-off frequency was selected to be nearly equal to the Kolmogorov frequency $f_K \equiv \langle U\rangle/2\pi\eta$ (0.83 kHz at $R_\lambda = 40$ and 13.9 kHz at $R_\lambda = 190$ and 230). The sampling frequency f_S was chosen to be $2f_K$ for $R_\lambda = 230$ but about $24f_K$ for $R_\lambda = 40$, the latter choice allowing good resolution ($\langle U\rangle f_S^{-1}/\eta \simeq 0.26$, where $\langle U\rangle$ is the local

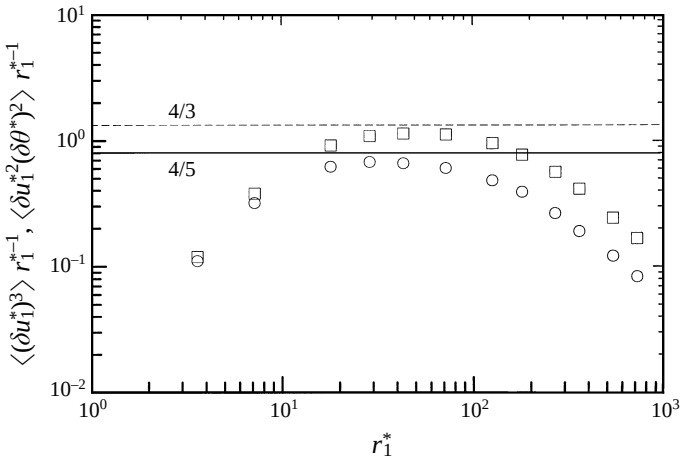

FIGURE 1. Distributions of $\langle(\delta u_1^*)^3\rangle r_1^{*-1}$ and $\langle \delta u_1^*(\delta\theta^*)^2\rangle r_1^{*-1}$ at $R_\lambda = 230$. ○, $\langle(\delta u_1^*)^3\rangle r_1^{*-1}$; □, $\langle(\delta u_1^*)(\delta\theta^*)^2\rangle r_1^{*-1}$; —, equation (1.2); - - -, equation (1.7).

mean velocity) of the dissipative scales. The selection of the cut-off frequency for the temperature signal was dictated in part by the frequency response of the cold wire and in part by the noise characteristics of the signal. The spectrum of $\partial\theta/\partial t$ was viewed on a Hewlett Packard spectrum analyser prior to selecting f_c; the procedure adopted was that outlined in Antonia, Satyaprakash & Hussain (1982). The final choice of f_c was about 8 kHz (f_c was set to 9.2 kHz for the u_1 signal which was sampled simultaneously with θ). The record duration was about 80 s, which is long enough for the mean, variance, skewness and kurtosis of u_i, θ, δu_i and $\delta\theta$ to converge to $\pm 5\%$ according to the criterion suggested by Antonia & Van Atta (1978).

5. Inertial-range results

The Kolmogorov-normalized third-order moments$\langle(\delta u_1^*)^3\rangle$ and $\langle(\delta u_1^*)(\delta\theta^*)^2\rangle$ are shown in figure 1 as a function of r_1^* for $R_\lambda = 230$. An asterisk denotes normalization by either the Kolmogorov velocity scale u_K, or the Kolmogorov (or Corrsin–Obukhov) temperature scale θ_K or the Kolmogorov length scale η. The moments in figure 1 have been multiplied by r_1^{*-1} to allow comparison with (1.2) and (1.7); these relations are often used as an indicator of the extent of the inertial range as well as a test for local isotropy in the inertial range. A modest plateau is indicated by the two data sets in figure 1. The extent of the plateau is approximately the same in each case but the magnitude of the plateau is smaller than 4/5 for $\langle(\delta u_1^*)^3\rangle$ and 4/3 for $\langle(\delta u_1^*)(\delta\theta^*)^2\rangle$. The values of $\langle\epsilon\rangle$ and $\langle\epsilon_\theta\rangle$ used for normalising the data in figure 1 were inferred from the isotropic relations (1.4) and (1.6). The results of figure 1 indicate that (1.2) and (1.7) yield values of $\langle\epsilon\rangle$ and $\langle\epsilon_\theta\rangle$ that are about 20% and 12% smaller than those estimated via (1.4) and (1.6).

There have been several experimental attempts to verify (1.2) and (1.7) using values of $\langle\epsilon\rangle$ and $\langle\epsilon_\theta\rangle$ estimated via (1.4) and (1.6). Although it is not our intent to review all these attempts in detail, it is reasonable to assert that typically the results fall into two categories. They either provide good support for (1.2) and/or (1.7) e.g. Park & Van Atta 1980; Antonia, Satyaprakash & Chambers 1982) or else they indicate that the values of $\langle\epsilon\rangle$ or $\langle\epsilon_\theta\rangle$ that satisfy (1.2) and (1.7) are somewhat smaller than those suggested by (1.4) and (1.6) (e.g. Zhu, Antonia & Hosokawa 1995; Saddoughi

& Veeravalli, 1994). There is no strong evidence to suggest that the magnitude of R_λ is responsible for the differences, when they occur. The atmospheric data of Zhu *et al.* (1995) were at a higher R_λ than those of Park & Van Atta (1980). In the jet experiment of Anselmet *et al.* (1984), (1.2) yielded a value of $\langle\epsilon\rangle$ which was about 12% smaller than that from (1.4) for $R_\lambda = 536$ but the two estimates were in good agreement for $R_\lambda = 852$. The Antonia *et al.* (1983) data on the centreline of a plane jet ($R_\lambda \simeq 160$) indicated good consistency between (1.6) and (1.7) but the value of $\langle\epsilon\rangle$ inferred from (1.2) was nearly 50% smaller than that obtained from (1.4). The agreement, when it occurs, between (1.2) and (1.4) or between (1.7) and (1.6), would imply that both dissipative scales (which make a major contribution to $\langle(\partial u_1/\partial x_1)^2\rangle$) and inertial-range scales are consistent with isotropy. While there is impressive evidence that small scales satisfy isotropy at least when the shear is small, there is only modest evidence that inertial scales conform with isotropy (the experiments of Saddoughi & Veeravalli suggest that inertial range isotropy becomes more tenable at large R_λ). Although it is difficult to accept that (1.4) and (1.6) can, in general, yield correct values of $\langle\epsilon\rangle$ and $\langle\epsilon_\theta\rangle$, there is no guarantee that (1.2) and (1.7) would result in more reliable values for these two quantities. Although $\langle(\partial u_1/\partial x_1)^2\rangle$ and $\langle(\partial\theta/\partial x_1)^2\rangle$ are more easily measured than the third-order moments in (1.2) and (1.7), the use of the latter equations may be more attractive as R_λ continues to increase, i.e. as the resolution of the small scales deteriorates. A calibration experiment, e.g. in grid turbulence where $\langle\epsilon\rangle$ and $\langle\epsilon_\theta\rangle$ can be estimated from the decay rates of the turbulent energy and temperature variance, would certainly be useful even if the large scales are nearly isotropic. The need to extend this calibration to non-homogeneous shear flows is all the more urgent when one recalls that, over the centreline region of a self-preserving wake, Browne, Antonia & Shah (1987) and Antonia & Browne (1986) found that the values of $\langle\epsilon\rangle$ from (1.4) and $\langle\epsilon_\theta\rangle$ from (1.6) are about 45% and 55% smaller than those estimated from measurements of the nine major terms that make up $\langle\epsilon\rangle$ and all three terms included in $\langle\epsilon_\theta\rangle$. The relevance of the Browne *et al.* result to the present wake experiment is not clear since R_λ was quite small ($\simeq 30$) for Browne *et al.* while the present wake flow has not yet reached self-preservation.

The third-order moment $\langle(\delta u_1^*)^3\rangle$ is replotted in figure 2 together with $\langle(\delta u_1^*)(\delta u_2^*)^2\rangle$ and $\langle(\delta u_1^*)(\delta u_3^*)^2\rangle$. The latter two quantities are approximately equal in the inertial range in support of the first equality in relation (2.11). Their numerical value in the inertial range is 4/15, as expected from isotropy, (1.2) and (2.11). The second equality in (2.11) is not quite satisfied since $\langle(\delta u_1^*)(\delta u_2^*)^2\rangle$ or $\langle(\delta u_1^*)(\delta u_3^*)^2\rangle$ is about 10% larger than $\frac{1}{3}\langle(\delta u_1^*)^3\rangle$. In the inertial range, the sum $\langle\delta u_1^*(\delta u_i^*)^2\rangle$ is somewhat smaller than the value of 4/3, given by (2.9). The distributions, as a function of r_1^*, for the three third-order moments in (2.11) were presented by Karyakin, Kuznetsov & Praskovsky (1991) using measurements in the return channel of the Central Aerohydrodynamic Institute of Moscow. These data (shown in figure 3) were obtained at $R_\lambda \simeq 3200$, i.e. one order of magnitude greater than in the present experiments. Correspondingly, the inertial range exhibited by $\langle(\delta u_1^*)^3\rangle$ or $\langle(\delta u_1^*)(\delta u_i^*)^2\rangle$ extends over one and a half decades of r_1^*. However, these quantities are smaller by about 12% and 15% respectively than the corresponding isotropic values. The two mixed third-order moments exhibit more scatter than $\langle(\delta u_1^*)^3\rangle$ and clearly show more departure from isotropy than the present data; the apparent rise at small r_1^* seems anomalous.

The present values of $\langle\delta u_1^*(\delta u_i^*)^2\rangle$ are plotted in figure 4 for comparison with $\langle\delta u_1^*(\delta\theta^*)^2\rangle$. There is close agreement between the two moments in the inertial range, in support of the analogy between (2.9) and (1.7). Also shown in figure 4 are data for $\langle\delta u_1^*(\delta u_i^*)^2\rangle$ obtained in the present flow at $R_\lambda = 190$ and in the Karyakin *et al.* (1991)

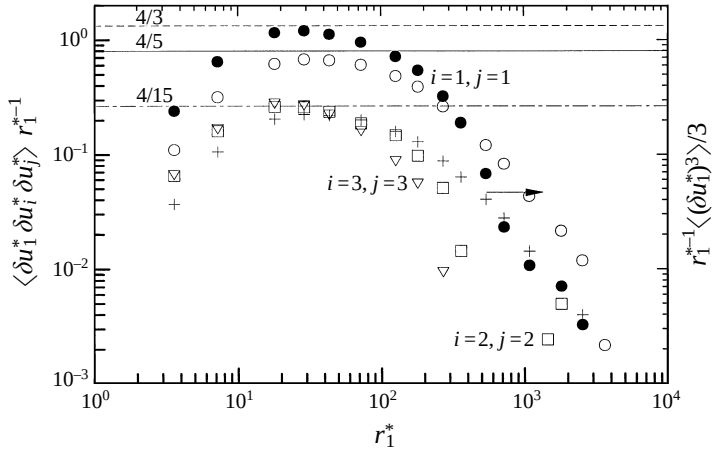

FIGURE 2. Third-order velocity structure functions. $R_\lambda = 230$. ○, $\langle (\delta u_1^*)^3 \rangle r_1^{*-1}$; □, $\langle \delta u_1^* (\delta u_2^*)^2 \rangle r_1^{*-1}$; ▽, $\langle \delta u_1^* (\delta u_3^*)^2 \rangle r_1^{*-1}$; ●, $\langle \delta u_1^* (\delta u_i^*)^2 \rangle r_1^{*-1}$; +, $1/3 \langle (\delta u_1^*)^3 \rangle r_1^{*-1}$; — - —, $\langle \delta u_1^* (\delta u_2^*)^2 \rangle r_1^{*-1} = \langle \delta u_1^* (\delta u_3^*)^2 \rangle r_1^{*-1} = 4/15$, namely (1.2) and (2.11); —, equation (1.2); - - -, equation (2.9).

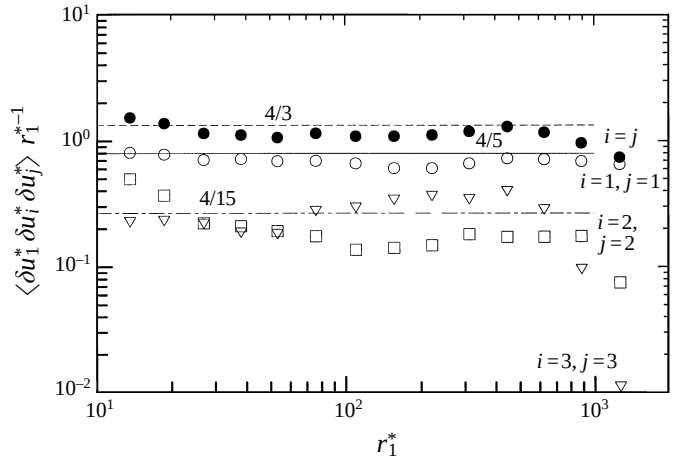

FIGURE 3. Third-order velocity structure functions measured by Karyakin *et al.* (1991). $R_\lambda = 3200$. ○, $\langle (\delta u_1^*)^3 \rangle r_1^{*-1}$; □, $\langle \delta u_1^* (\delta u_2^*)^2 \rangle r_1^{*-1}$; ▽, $\langle \delta u_1^* (\delta u_3^*)^2 \rangle r_1^{*-1}$; ●, $\langle \delta u_1^* (\delta u_i^*)^2 \rangle r_1^{*-1}$; — - —, $\langle \delta u_1^* (\delta u_2^*)^2 \rangle r_1^{*-1} = \langle \delta u_1^* (\delta u_3^*)^2 \rangle r_1^{*-1} = 4/15$, namely (1.2) and (2.11); —, equation (1.2); - - -, equation (2.9).

wind tunnel at $R_\lambda = 3200$ as well as atmospheric data for $\langle \delta u_1^* (\delta \theta^*)^2 \rangle$ at $R_\lambda = 7200$ (details for the latter data are given in Zhu *et al.* 1995). The trend of the three data sets for $\langle \delta u_1^* (\delta u_i^*)^2 \rangle$ supports the notion that an inertial range with the same numerical value is established in each case although its extent clearly increases with R_λ. The two data sets for $\langle \delta u_1^* (\delta \theta^*)^2 \rangle$ are also consistent with the increased extent of the inertial range as R_λ increases. Further, the approximate equality between $\langle \delta u_1^* (\delta \theta^*)^2 \rangle$ and $\langle \delta u_1^* (\delta u_i^*)^2 \rangle$ in the inertial range is validated rather impressively when R_λ is large.

The equality $\langle \delta u_1^* (\delta \theta^*)^2 \rangle = \langle \delta u_1^* (\delta u_i^*)^2 \rangle$ or, equivalently,

$$\langle \epsilon \rangle / \langle \epsilon_\theta \rangle = \langle \delta u_1 (\delta u_i)^2 \rangle / \langle \delta u_1 (\delta \theta)^2 \rangle, \tag{5.1}$$

implies that $\langle \epsilon \rangle$ could be estimated once the other three quantities in (5.1) are known.

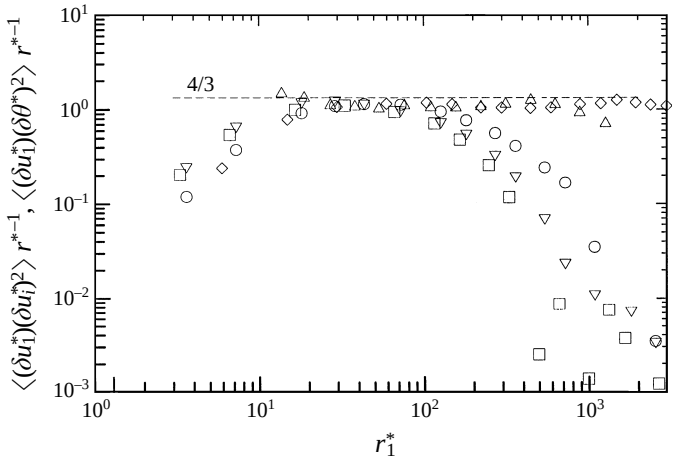

FIGURE 4. Comparison between (1.7) and (2.9) and different values of R_λ. $\langle\delta u_1^*(\delta u_i^*)^2\rangle r_1^{*-1}$: □, present, $R_\lambda = 190$; ▽, present, $R_\lambda = 230$; △, Karyakin *et al.* (1991), $R_\lambda = 3200$. $\langle\delta u_1^*(\delta\theta^*)^2\rangle r_1^{*-1}$: ○, present $R_\lambda = 230$; ◇, Zhu *et al.* (1995), $R_\lambda = 7200$.

In this context, both $\langle\delta u_1(\delta u_i)^2\rangle$ and $\langle\delta u_1(\delta\theta)^2\rangle$ can be determined from a X-wire/cold wire combination while $\langle\epsilon_\theta\rangle$ can be determined relatively accurately using a pair of parallel cold wires (the three components of $\langle\epsilon_\theta\rangle$ can be estimated by either a finite difference method or a two-point correlation method).

Whether this approach, which is considerably more involved than simply using (1.2) or (1.4), is warranted remains to be validated, especially since isotropic estimates of $\langle\epsilon\rangle$ and $\langle\epsilon_\theta\rangle$ were used in figure 4. The relation

$$\langle\epsilon\rangle/\langle\epsilon_\theta\rangle = R\langle q^2\rangle/\langle\theta^2\rangle, \tag{5.2}$$

which is the definition of the time scale ratio R (e.g. Béguier, Dekeyser & Launder 1978), provides an attractive means of estimating $\langle\epsilon\rangle$ when R (a constant, typically $\simeq 0.5$), $\langle\theta^2\rangle$, $\langle q^2\rangle$ and $\langle\epsilon_\theta\rangle$ are known. There seems little doubt however that (5.1) has a much stronger theoretical basis than (5.2). It could also be argued that (5.2) would have a much smaller claim to universality than (5.1) since the third-order moments which feature in (5.1) are less likely to feel the influence of initial conditions than the variances in the right-hand side of (5.2). The inertial-range behaviours of $\langle(\delta u_1)(\delta u_i)^2\rangle$ and $\langle(\delta u_1)(\delta\theta)^2\rangle$ are not affected by the intermittency of the dissipation fields. Frisch (1995) noted that the four-fifths law constitutes a kind of boundary condition, presumably in the sense of a constant, on theories of turbulence; obviously, the same can be said about the four-thirds laws represented by (2.9) and (1.7).

6. Dissipation-range results

In this section, we consider the limiting forms of (2.8) and (1.5) when r_1 tends to zero. The results, given by (2.10) and (1.8) respectively, can be rewritten in normalized form:

$$\left\langle \left(\frac{\partial u_1^*}{\partial x_1^*}\right)\left(\frac{\partial u_i^*}{\partial x_1^*}\right)^2 \right\rangle = -\frac{2}{3}\left\langle \left(\frac{\partial^2 u_i^*}{\partial x_1^{*2}}\right)^2 \right\rangle, \tag{6.1}$$

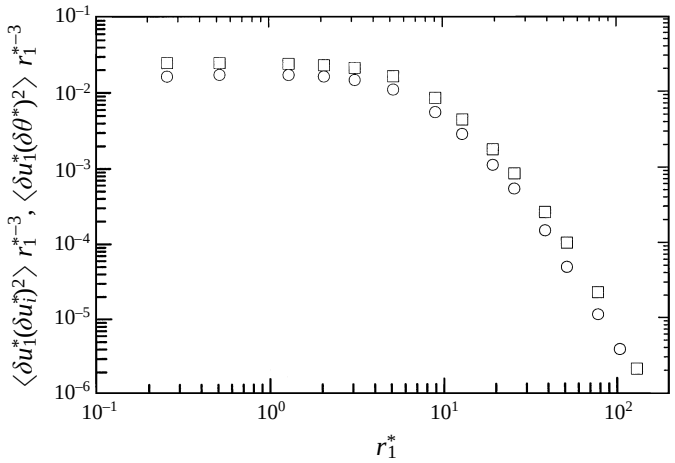

FIGURE 5. Behaviour of $\langle \delta u_1^*(\delta u_i^*)^2 \rangle$ and $\langle \delta u_1^*(\delta\theta^*)^2 \rangle$ for small separations. $R_\lambda = 40$. ○, $\langle \delta u_1^*(\delta u_i^*)^2 \rangle r_1^{*-3}$; □, $\langle \delta u_1^*(\delta\theta^*)^2 \rangle r_1^{*-3}$.

	Measured value	Isotropic value	Discrepancy between measured and isotropic values
$\langle {u_{1,1}^*}^2 \rangle$	0.067	0.067	†
$\langle {u_{2,1}^*}^2 \rangle$	0.122	$2\langle {u_{1,1}^*}^2 \rangle = 0.14$	–15%
$\langle {u_{3,1}^*}^2 \rangle$	0.121	$2\langle {u_{1,1}^*}^2 \rangle = 0.14$	–16%
$\langle {\theta_{,1}^*}^2 \rangle$	0.1975	—	—
$\langle {u_{1,11}^*}^2 \rangle$	0.0047	—	—
$\langle {u_{2,11}^*}^2 \rangle$	0.015	$3\langle {u_{1,11}^*}^2 \rangle = 0.014$	+7%
$\langle {u_{3,11}^*}^2 \rangle$	0.014	$3\langle {u_{1,11}^*}^2 \rangle = 0.014$	0%
$\langle {u_{i,11}^*}^2 \rangle$	0.0337	$7\langle {u_{1,11}^*}^2 \rangle = 0.0329$	+2%
$\langle {\theta_{,11}^*}^2 \rangle$	0.026	—	—
$\langle {u_{1,1}^*}^3 \rangle$	9.83×10^{-3}	—	—
$\langle u_{1,1}^* {u_{2,1}^*}^2 \rangle$	4.41×10^{-3}	$(2/3)\langle {u_{1,1}^*}^3 \rangle = 6.55 \times 10^{-3}$	–49%
$\langle u_{1,1}^* {u_{3,1}^*}^2 \rangle$	3.17×10^{-3}	$(2/3)\langle {u_{1,1}^*}^3 \rangle = 6.55 \times 10^{-3}$	–107%
$\langle u_{1,1}^* {u_{i,1}^*}^2 \rangle$	0.0174	$-(2/3)\langle {u_{i,11}^*}^2 \rangle = 0.0225$	–29%
$\langle u_{1,1}^* {\theta_{,1}^*}^2 \rangle$	0.0245	$-(2/3Pr)\langle {\theta_{,11}^*}^2 \rangle = 0.0237$	3%

† This comparison is not meaningful since estimates of u_K and η are based on isotropic values of $\langle \epsilon \rangle$.

TABLE 2. Derivative Statistics for $R_\lambda = 40$ and Comparison with Isotropy. (All quantities are normalized by Kolmogorov scales; in this table, a more economic notation has been used for denoting derivatives, e.g. $u_{1,1} \equiv \partial u_1/\partial x_1$ and $u_{1,11} \equiv \partial^2 u_1/\partial x_1^2$).)

$$\left\langle \left(\frac{\partial u_1^*}{\partial x_1^*}\right) \left(\frac{\partial \theta^*}{\partial x_1^*}\right)^2 \right\rangle = -\frac{2}{3}\,\frac{1}{Pr} \left\langle \left(\frac{\partial^2 \theta^*}{\partial x_1^{*2}}\right)^2 \right\rangle. \tag{6.2}$$

The left-hand sides of (6.1) and (6.2) represent the limiting values of $\langle \delta u_1^*(\delta u_i^*)^2 \rangle / r_1^{*3}$ and $\langle \delta u_1^*(\delta\theta^*)^2 \rangle / r_1^{*3}$ as $r_1^* \to 0$. The data in figure 5 indicate that these two quantities asymptote to constant values for $r_1^* \lesssim 1$ (the smallest value of r_1^* is about 0.25,

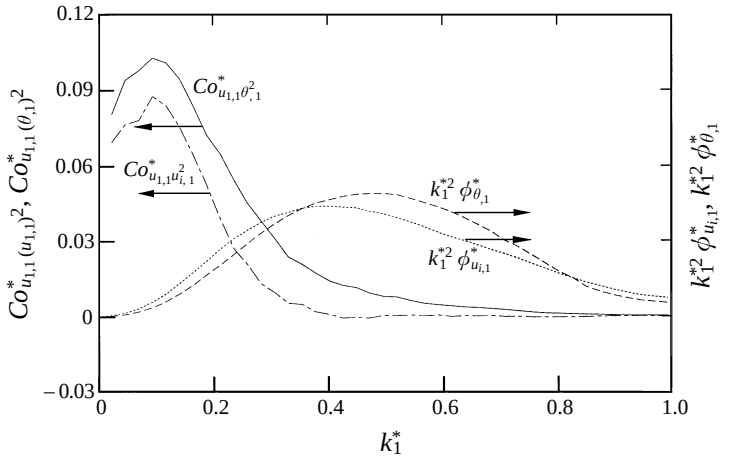

FIGURE 6. Spectral distributions corresponding to left- and right-hand sides of (6.1) and (6.2). $R_\lambda = 40$. The areas under the cospectra are equal to the left-hand sides of (6.1) and (6.2). The areas under $k_1^{*2}\phi^*_{u_{i,1}}$ and $k_1^{*2}\phi^*_{\theta,1}$ are equal to the right-hand sides of (6.1) and (6.2). —, $Co^2_{u_{1,1}\theta^*_{,1}}$; — - —, $Co^*_{u_{1,1}u^2_{i,1}}$; - - -, $k_1^{*2}\phi^*_{\theta,1}$; $\cdots$, $k_1^{*2}\phi^*_{u_{i,1}}$.

reflecting the good spatial resolution of the present experiment for $R_\lambda = 40$). The constant values (0.018 and 0.024 respectively) agree to within 3% with estimates of these two quantities (table 2) obtained directly from the time series of $\partial u_1/\partial t$, $\partial u_2/\partial t$, $\partial u_3/\partial t$ and $\partial\theta/\partial t$. The values of $\langle(\partial^2 u_i^*/\partial x_1^{*2})^2\rangle$ and $\langle(\partial^2\theta^*/\partial x_1^{*2})^2\rangle$, which appear on the right-hand sides of (6.1) and (6.2), were inferred from Kolmogorov-normalized spectra of the time derivatives $\partial u_i/\partial t$ $(i = 1, 2, 3)$ and $\partial\theta/\partial t$. These spectra were multiplied by k_1^{*2}, where k_1 is the one-dimensional wavenumber, and integrated with respect to k_1^* from $k_1^* = 0$ to $k_1^* = 1$.† The resulting values (0.0337 and 0.026, see table 2) imply that the equalities expressed by (6.1) and (6.2) are satisfied to within 29% and 3% respectively (table 2). While these results imply that isotropy is not as well satisfied for velocity as for temperature, it should be noted that the second-order derivatives on the right-hand sides of (6.1) and (6.2) weight small scales more than the third-order moments on the left-hand sides of these equations. This is reflected in the separations between the peaks of the cospectra and the second-order derivative spectra shown in figure 6. In this figure, the notation is such that $Co^*_{u_{1,1}\theta^2_{,1}}$ is the Kolmogorov-normalized cospectrum between $(\partial u_1/\partial x_1)$ and $(\partial\theta/\partial x_1)^2$ while $\phi^*_{\theta,1}$ is the Kolmogorov-normalized spectrum of $(\partial\theta/\partial x_1)$. The present data for $\langle(\partial^2 u_1/\partial x_1^2)^2\rangle$, $\langle(\partial^2 u_2/\partial x_1^2)^2\rangle$ and $\langle(\partial^2 u_3/\partial x_1^2)^2\rangle$ (table 2) satisfy relation (2.12) quite well, which therefore suggests that isotropy of the small-scale velocity field is not violated in the present flow, despite the small value of R_λ. Equation (2.13) indicates that, for isotropy, $\langle(\partial u_1/\partial x_1)(\partial u_2/\partial x_1)^2\rangle$ and $\langle(\partial u_1/\partial x_1)(\partial u_3/\partial x_1)^2\rangle$ should be equal. The present data suggest (table 2) that these terms are 49% and 107% smaller than the value of $\frac{2}{3}(\langle(\partial u_1/\partial x_1)^3\rangle)$, the third term in (2.13). The discrepancies are large and consistent with the expectation that the cospectrum, which is largest at

† This procedure is equivalent to using the sum of the spectra of the three velocity components and the temperature spectrum and multiplying these by k_1^{*4} before integrating. The present approach was preferred because spectra of derivatives were less affected by noise than those of the undifferentiated signals.

relatively low wavenumbers, is more likely to be affected by the anisotropy of the large scales. They are also consistent with the observation that cospectra (not shown here) between $\partial u_1/\partial x_1$ and either $(\partial u_2/\partial x_1)^2$ or $(\partial u_3/\partial x_1)^2$ change sign for $k_1^* \gtrsim 0.25$. The ratio $\langle(\partial u_1^*/\partial x_1^*)^3\rangle/2\langle(\partial^2 u_1^*/\partial x_1^{*2})^2\rangle$ is 1.05, i.e. (1.3) is satisfied to an accuracy (5%) comparable to that reported in previous studies (e.g. Antonia, Anselmet & Chambers 1986; Kim & Antonia 1993).

7. Conclusions and final discussion

It is generally accepted that the quantities $\langle(\delta u_1)^3\rangle$ and $\langle(\delta u_1)(\delta\theta)^2\rangle$ are important in view of their direct connection to the transfer rates of $(\delta u_1)^2$ and $(\delta\theta)^2$ from large to small scales. For example, Frisch, Sulem & Nelkin (1978) and Anselmet *et al.* (1984) argued that $(\delta u_1)^3/r_1$ represents the dissipation of $(\delta u_1)^2$ over a time of order $r_1/(\delta u_1)$, i.e. typically the eddy turnover time. Similarly, Antonia *et al.* (1984) suggested that $\delta u_1(\delta\theta)^2/r_1$ represents the dissipation of $(\delta\theta)^2$ over a time of order $r_1/(\delta u_1)$. The Kolmogorov and Yaglom equations in which $\langle(\delta u_1)^3\rangle$ and $\langle\delta u_1(\delta\theta)^2\rangle$ appear have provided a benchmark for small-scale turbulence models and measurements since they indicate that these third-order moments are not affected by the small-scale intermittency. In the present paper, we have indicated that it is more proper – both physically and mathematically – to compare $\langle\delta u_1(\delta\theta)^2\rangle$ with $\langle\delta u_1(\delta u_i)^2\rangle$ than with $\langle(\delta u_1)^3\rangle$ and have shown that Kolmogorov's equation can be generalized, albeit within the framework of isotropy, to a transport equation for $\langle(\delta u_i)^2\rangle$. The close similarity between (2.9) and (1.7) reflects the fact that the scalar fluctuation is transported by the fluctuating velocity vector (e.g. Batchelor 1959) and not just the longitudinal component of this vector. The close similarity in the inertial range between the third-order moments $\langle\delta u_1(\delta u_i)^2\rangle$ and $\langle\delta u_1(\delta\theta)^2\rangle$ extends the previously established similarity (Antonia *et al.* 1996), also in the inertial range, between $\langle(\delta u_i)^2\rangle$ and $\langle(\delta\theta)^2\rangle$ or, equivalently, the spectral analogy between the spectra corresponding to u_i^2 originally proposed by Fulachier (1972) and Fulachier & Dumas (1976). These authors (see also Fulachier & Antonia, 1984) argued that the transport equations for $\langle u_i(\boldsymbol{x}_0)u_i(\boldsymbol{x})\rangle$ and $\langle\theta(\boldsymbol{x}_0)\theta(\boldsymbol{x})\rangle$ are analogous in the case of homogeneous turbulence. Only homogeneity was required to derive (2.6) and (3.6), which are also analogous. The assumption of isotropy, which is made only to project these two equations onto the r_1-direction, would therefore appear to be a weak assumption. Although (1.2), (1.7) and (2.9) assume isotropy at all scales, it is not unreasonable to expect that, when R_λ is sufficiently large and the mean shear is sufficiently small, inertial-range scales will not deviate significantly from isotropy. It remains to be explored whether the assumption of axisymmetry, which is less restrictive than isotropy but more constraining than homogeneity, is sufficient for establishing (2.8) and (1.5).

The similarity between (2.9) and (1.7) is well supported by the present wake data at $R_\lambda = 230$ for inertial-range separations. The atmospheric data for $\langle\delta u_1(\delta\theta)^2\rangle$ and the high-R_λ data for $\langle\delta u_1(\delta u_i)^2\rangle$ obtained in a large-scale facility (Karyakin *et al.* 1991) confirm this similarity over an extended inertial range. The similarity implies that the average dissipation rates of turbulent kinetic energy and half the temperature variance are simply related via the ratio $\langle\delta u_1(\delta u_i)^2\rangle/\langle\delta u_1(\delta\theta)^2\rangle$, i.e. (5.1), for inertial-range separations. This latter relation should be more rigorous and have wider applicability than (5.2), which is based on the definition of the dissipation time-scale ratio.

The similarity between (2.10) and (1.8) is in good accord with the data at $R_\lambda = 40$. Figures 5 and 6 confirm that the similarity between $\langle\delta u_1(\delta u_i)^2\rangle$ and $\langle\delta u_1(\delta\theta)^2\rangle$ also

applies to small scales. In particular, figure 6 provides a more adequate comparison, both in terms of shape and magnitude, between the major terms in the equations for the mean-square vorticity and the mean-square temperature gradient. This further supports the main contribution of this paper, namely a more general form of Kolmogorov's equations, specifically one which describes more fully the transport of turbulent energy in different size eddies, provides a better basis of comparison with Yaglom's equation.

The support of the Australian Research Council is gratefully acknowledged. R. A. A. is grateful for the hospitality he enjoyed at the IRPHE while on study leave there on a CNRS Poste Rouge Award. A debt of thanks is owed Dr L. Fulachier for many interesting discussions and his support of this work. We also would like to acknowledge useful comments from three referees.

REFERENCES

Anselmet, F., Gagne, Y., Hopfinger, E. J. & Antonia, R. A. 1984 High-order velocity structure functions in turbulent shear flows. *J. Fluid Mech.* **140**, 63–89.

Antonia, R. A., Anselmet, F. & Chambers, A. J. 1986 Assessment of local isotropy using measurements in a turbulent plane jet. *J. Fluid Mech.* **163**, 365–391.

Antonia, R. A. & Browne, L. W. B. 1986 Anisotropy of the temperature dissipation in a turbulent wake. *J. Fluid Mech.* **163**, 393–403.

Antonia, R. A., Chambers, A. J. & Browne, L. W. B. 1983 Relations between structure functions of velocity and temperature in a turbulent jet. *Exps. Fluids* **1**, 213–219.

Antonia, R. A., Hopfinger, E. J., Gagne, Y. & Anselmet, F. 1984 Temperature structure functions in turbulent shear flows. *Phys. Rev.* A **30**, 2704–2707.

Antonia, R. A. & Kim, J. 1994 A numerical study of local isotropy of turbulence. *Phys. Fluids* A **6**, 834–841.

Antonia, R. A., Satyaprakash, B. R. & Chambers, A. J. 1982 Reynolds number dependence of velocity structure functions in turbulent shear flows. *Phys. Fluids* **25**, 29–37.

Antonia, R. A., Satyaprakash, B. R. & Hussain, A. K. M. F. 1982 Statistics of fine scale velocity in turbulent plane and circular jets. *J. Fluid Mech.* **119**, 55–89.

Antonia, R. A. & Van Atta, C. W. 1978 Structure functions of temperature fluctuations in turbulent shear flows. *J. Fluid Mech.* **84**, 561–580.

Antonia, R. A., Zhu, Y., Anselmet, F. & Ould-rouis, M. 1996 Comparison between the sum of the second-order velocity structure functions and the second-order temperature structure functions. *Phys. Fluids* **8**, 3105–3111.

Batchelor, G. K. 1947 Kolmogoroff's theory of locally isotropic turbulence. *Proc. Camb. Phil. Soc.* **43**, 553–559.

Batchelor, G. K. 1959 Small-scale variation of convected quantities like temperature in turbulent fluid. Part 1. General discussion and the case of small conductivity. *J. Fluid Mech.* **5**, 113–133.

Batchelor, G. K. & Townsend, A. A. 1947 Decay of vorticity in isotropic turbulence. *Proc. R. Soc. Lond.* A **190**, 543–550.

Béguier, C., Dekeyser, I. & Launder, B. E. 1978 Ratio of scalar and velocity dissipation time scales in shear flow turbulence. *Phys. Fluids* **21**, 307–310.

Browne, L. W. B., Antonia, R. A. & Shah, D. A. 1987 Turbulent energy dissipation in a wake. *J. Fluid Mech.* **179**, 307–326.

Champagne, F. H. 1978 The fine-scale structure of the turbulent velocity field. *J. Fluid Mech.* **86**, 67–108.

Durbin, P. A. & Speziale, C. G. 1991 Local anisotropy in strained turbulence at high Reynolds numbers. *Trans. ASME J. Fluids Engng* **113**, 707.

Frisch, U. 1995 *Turbulence : The Legacy of A. N. Kolmogorov*. Cambridge University Press.

Frisch, U., Sulem, P.-L. & Nelkin, M. 1978 A simple dynamical model of intermittent fully developed turbulence. *J. Fluid Mech.* **87**, 719–736.

Fulachier, L. 1972 Contribution à l'étude des analogies des champs dynamique et thermique dans une couche limite turbulente — effet de l'aspiration. Thèse Docteur ès Sciences Physiques, Université de Provence.

Fulachier, L. & Antonia, R. A. 1984 Spectral analogy between temperature and velocity fluctuations in several turbulent flows. *Intl J. Heat Mass Transfer* **27**, 987–997.

Fulachier, L. & Dumas, R. 1976 Spectral analogy between temperature and velocity fluctuations in a turbulent boundary layer. *J. Fluid Mech.* **77**, 257–277.

Hinze, J. O. 1959 *Turbulence*. McGraw-Hill.

Kármán, T. von & Howarth, L. 1938 On the statistical theory of isotropic turbulence. *Proc. R. Soc. Lond.* A **164**, 192–215.

Karyakin, M. Yu., Kuznetsov, V. R. & Praskovsky, A. A. 1991 Experimental verification of the hypothesis of fine-scale isotropy of turbulence. *Fluid Dyn. Res.* **26**, 658–670.

Kim, J. & Antonia, R. A. 1993 Isotropy of the small scales of turbulence at low Reynolds number. *J. Fluid Mech.* **251**, 219–238.

Kolmogorov, A. N. 1941 Energy dissipation in locally isotropic turbulence. *Dokl. Akad. Nauk SSSR* **32**, 19–21.

Landau, L. D. & Lifshitz, E. M. 1987 *Fluid Mechanics*, 2nd edn. Pergamon Press.

Lindborg, E. 1996 Studies in classical turbulence theory. PhD Thesis, Royal Institute of Technology, Stockholm.

Monin, A. S. 1959 On the theory of locally isotropic turbulence. *Dokl. Akad. Nauk SSSR* **125**, 515–518.

Monin, A. S. & Yaglom, A. M. 1975 *Statistical Fluid Mechanics*. MIT Press.

Nelkin, M. 1994 Universality and scaling in fully developed turbulence. *Adv. Phys.* **43**, 143–181.

Park, J. T. & Van Atta, C. W. 1980 Hot- and cold-wire sensitivity corrections for moments of the fine scale turbulence in heated flows. *Phys. Fluids* **23**, 701–705.

Saddoughi, S. G. & Veeravalli, S. F. 1994 Local isotropy in turbulent boundary layers at high Reynolds number. *J. Fluid Mech.* **268**, 333–372.

Shah, D. A. & Antonia, R. A. 1986 Isotropic forms of vorticity and velocity structure function equations in several turbulent shear flows. *Phys. Fluids* **29**, 4016–4024.

Vainshtein, S. I. & Sreenivasan, K. R. 1994 Kolmogorov's $4/5^{th}$ law and intermittency in turbulence. *Phys. Rev. Lett.* **73**, 3085–3088.

Wyngaard, J. C. 1971 The effect of velocity sensitivity on temperature derivative statistics in isotropic turbulence. *J. Fluid Mech.* **48**, 763–769.

Yaglom, A. M. 1949 On the local structure of a temperature field in a turbulent flow. *Dokl. Akad. Nauk SSSR* **69**, 743–746.

Zhu, Y., Antonia, R. A. & Hosokawa, I. 1995 Refined similarity hypothesis for turbulent velocity and temperature fields. *Phys. Fluids* **7**, 1637–1648.